Three-nucleon force effects in nucleon-deuteron scattering at backward angles

Souichi Ishikawa[⋆]

Hosei University, Tokyo, Japan

⋆ ishikawa@hosei.ac.jp

Abstract

Elastic and breakup cross sections in nucleon-deuteron scattering at intermediate energies are calculated using a realistic two-nucleon potential and three-nucleon potentials based on the exchange of two pions among three nucleons. Attractive effects of the pion-exchange at medium range region in the three-nucleon potential are recovered by using a shorter range cutoff. It is shown that these effects increase the cross sections at backward angles, which tends to reduce discrepancies between theoretical calculations and experimental data.

1 Introduction

The necessity of three-nucleon potentials (3NPs) in the nuclear Hamiltonian in addition to two-nucleon potentials (2NPs) is well recognized. However our understanding of 3NPs is quite incomplete except the 3NP based on Fig. 1, namely two-pion exchange process among three nucleons (2πE), and then combinations of a 2NP model and a 2πE-3NP model have been often used in few-nucleon calculations.

In spite of various successful 2πE-3NP effects on 3N observables, there are still unsolved discrepancies between experimental data and calculations. A typical example is the differential cross sections at backward angles of nucleon-deuteron (Nd) elastic scattering for intermediate energy.

It is noticed that the 2πE-3NP has quite large attractive character, which should be suppressed by introducing a cutoff procedure to reproduce three-nucleon (3N) binding energies. Since it turns out that the range of the cutoff is not limited to a short range, effects of the pion-exchange process in 3NP may be eliminated even at rather longer distances. Thus, this ad hoc cutoff procedure might affect 3N observables such as ND elastic cross sections at backward angles. In this work, Nd cross sections are studied using Hamiltonian models consisting of a

two-nucleon potential and 2πE-3NPs with a rather short range cutoff by adding phenomenological repulsive 3NPs as a counterpart [1].

In Sec. 2, a short note on numerical calculations and nuclear interaction models used in this work will be given. Results of calculations will be presented in Sec. 3, and conclusion will be given in Sec. 4.

2 Method and models

2.1 Three-nucleon Faddeev calculations

Three-body calculations in the present paper are performed by solving the Faddeev equations [2] as integral equations in coordinate space using a method developed in Ref. [3].

3N partial wave states for which 2NPs and 3NPs act, are restricted to those with total two-nucleon angular momenta $j \leq 6$ for bound state calculations, and $j \leq 5$ for scattering state calculations. For scattering state calculations, 3N partial wave states with the total 3N angular momentum $J \leq 27/2$ are taken into account, while 3NPs are switched on for 3N states with $J \leq 13/2$.

2.2 Two-pion exchange three-nucleon potential

The momentum space representation of a component of the 2πE-3NP described by the diagram, Fig. 1, is given by

$$
\begin{aligned}
\hat{V}^{(3:1,2)}(\vec{q}_1, \vec{q}_2) &= \frac{1}{(2\pi)^6} \left(\frac{g_A}{2f_\pi} \right)^2 \frac{1}{\vec{q}_1^2 + m_\pi^2} \frac{1}{\vec{q}_2^2 + m_\pi^2} (\vec{\sigma}_1 \cdot \vec{q}_1)(\vec{\sigma}_2 \cdot \vec{q}_2) \\
&\times \left[(\vec{\tau}_1 \cdot \vec{\tau}_2)\{a + b(\vec{q}_1 \cdot \vec{q}_2)\} + (i\vec{\tau}_3 \cdot \vec{\tau}_1 \times \vec{\tau}_2)(i\vec{\sigma}_3 \cdot \vec{q}_1 \times \vec{q}_2)d \right], \quad (1)
\end{aligned}
$$

where momentum $\vec{q}_i$ $(i = 1, 2)$ is defined in Fig. 1, m_π is the pion mass, $\vec{\sigma}_i$ $(\vec{\tau}_i)$ is spin (isospin) operator of the nucleon i, g_A is the axial charge of the nucleon, and f_π is the pion decay constant. The coefficients, a, b, and d, characterize the 2πE-3NP, which are extracted from pion-nucleon scattering amplitudes. In this paper, I will use a newer version of the Brazil 2πE-3NP, BR-$\mathcal{O}(q^4)$ in Ref. [4] (BR07), whose coefficients are

$$
(a, b, d) = \left(0.981 m_\pi^{-1}, -2.617 m_\pi^{-3}, -0.854 m_\pi^{-3} \right).
$$

The coordinate space representation of the 2πE-3NP is given by

$$
V^{(3:1,2)}(\vec{r}_{13}, \vec{r}_{23}) = \int d\vec{q}_1 d\vec{q}_2 e^{-i\vec{q}_1 \cdot \vec{r}_{13} - i\vec{q}_2 \cdot \vec{r}_{23}} F_\Lambda(\vec{q}_1^2) F_\Lambda(\vec{q}_2^2) \hat{V}^{(3:1,2)}(\vec{q}_1, \vec{q}_2), \quad (2)
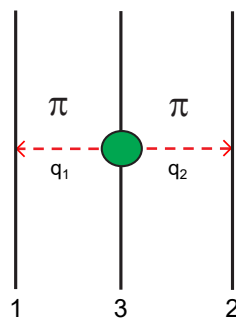$$

Figure 1: Diagram that shows a component of the 2πE-3NP. Total 2πE-3NP is the sum of cyclic permutations of this diagram.

Table 1: Empirical and calculated values of the ^{3}He binding energy and strength parameter V_C of the additional C-3NP, Eq. (4), for models used in this paper. See the text for the description of the models.

Model	V_C (MeV)	BE(^{3}He) (MeV)
Empirical		7.718
AV18		6.928
+BR$_{660}$		7.763
+BR(C)$_{1000}$	139	7.727
+BR$_{[I]0.87}$		7.718
+BR(C)$_{[I]0.5}$	159	7.726
+BR$_{[II]1.29}$		7.719
+BR(C)$_{[II]0.75}$	160	7.716

where $\vec{r}_{ij} = \vec{r}_i - \vec{r}_j$, and $F_\Lambda\left(\vec{q}^2\right)$ is a form factor. I this work, I will take a dipole form:

$$F_\Lambda\left(\vec{q}^2\right) = \left(\frac{\Lambda^2 - m_\pi^2}{\Lambda^2 + \vec{q}^2}\right)^2. \tag{3}$$

Here, the parameter Λ represents a scale of the cutoff momentum of the exchanged pions. Calculations with the BR07-3NP adapting the dipole form factor with the cutoff parameter Λ will be denoted as BR$_\Lambda$.

In the present paper, I will use the Argonne V$_{18}$ (AV18) 2NP model [5]. Calculated ^{3}He binding energy for the AV18 are shown in Table 1, which indicates the AV18 calculation underbinds the ^{3}He bound state by about 0.8 MeV. When the BR07-3NP is combined with the AV18-2NP, the cutoff parameter Λ determined to reproduce the ^{3}He binding energy is $\Lambda = 660$ MeV (BR$_{660}$) (see Table 1 for numerical values). This value of Λ is quite small compared with ones used in one-boson exchange 2NP models, such as the CD-Bonn potential [6], which are larger than 1000 MeV. This indicates that some medium range contributions in 2πE-3NP may be reduced.

3 Calculations

3.1 Elastic cross sections

In Fig. 2 (a) and (b), calculations of differential cross section for elastic proton-deuteron (p-d) scattering at $E_p = 65$ MeV and $E_p = 170$ MeV, respectively, are compared with experimental data [7,8]. In the figures, AV18 and AV18+BR$_{660}$ calculations are shown by black and red curves, respectively, which demonstrates that the deviations between the AV18 calculations and the data, especially at the minimum region, $90° < \theta < 150°$, are well reduced by introducing the BR$_{660}$ for $E_p = 65$ MeV, but is not enough for $E_p = 170$ MeV.

Here, I remark that the momentum transfer from the incident proton to deuteron, which is calculated from the scattering angle, exceeds the value of 660 MeV/c for scattering angles larger than 120° for $E_p = 170$ MeV. Thus, effects of the pion exchange in 2πE-3NP at large scattering angles might be suppressed by using the cutoff parameter of 660 MeV.

Next, I will examine the BR07-3NP with a large value of Λ, namely 1000 MeV. When the cutoff mass Λ larger than 660 MeV is used, calculated ^{3}He binding energy for AV18 + BR$_\Lambda$ are too large. In order to reproduce the ^{3}He binding energy, I introduce a spin-independent
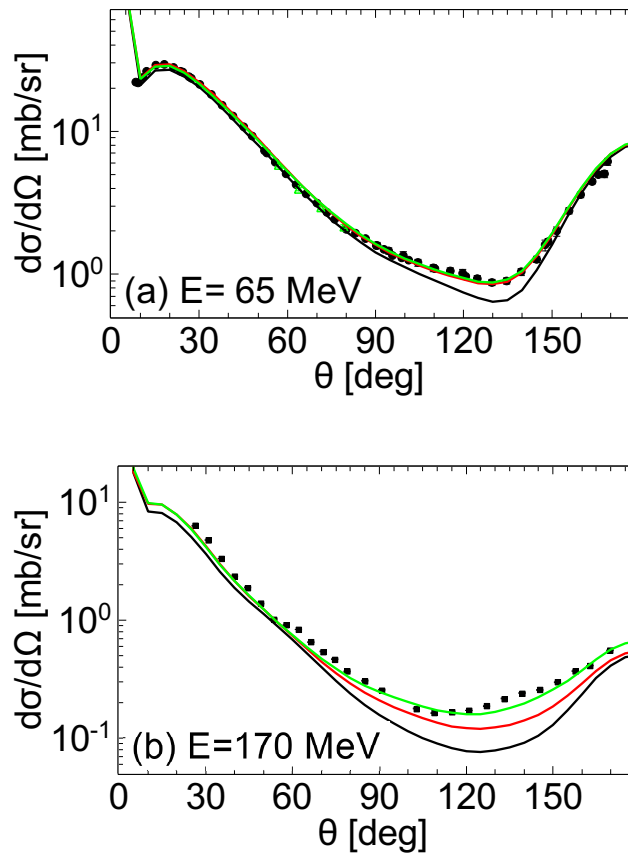
Figure 2: Cross sections for p-d elastic scattering at (a) $E_p = 65$ MeV and (b) $E_p = 170$ MeV. Black, red, and green curves denote AV18, AV18+BR$_{660}$, and AV18+BR(C)$_{1000}$ calculations, respectively. Experimental data are taken from Ref. [7] for $E_p = 65$ MeV and Ref. [8] for $E_p = 170$ MeV.

repulsive Gaussian 3NP [9], which will be denoted as C-3NP:

$$W_C = V_C \sum_{cyclic} e^{-(\frac{r_{ik}}{r_C})^2 - (\frac{r_{jk}}{r_C})^2}, \tag{4}$$

where r_{ij} is the relative distance between nucleons i and j, r_C the range parameter, and V_C the strength parameter. With fixing $r_C = 1.0$ fm, fitted value of V_C for $\Lambda = 1000$ MeV is shown as BR(C)$_{1000}$ in Table 1.

In Fig. 2, calculations of AV18+BR(C)$_{1000}$ are shown by green curves, which demonstrates that the introduction of the BR(C)$_{1000}$ gives almost the same effect on the cross section as BR$_{660}$ at $E_p = 65$ MeV, while increases the cross section at backward angles larger than BR$_{660}$ to give a reasonable agreement with the data at $E_p = 170$ MeV.

3.2 Inclusive breakup cross section

Next, I will study the effect of a large cutoff parameter in the 2πE-3NP on deuteron breakup reactions, $p + d \rightarrow p + p + n$. Since there are large numbers of configurations for final three-nucleon states, here, I just pick up an inclusive breakup reaction, ^{2}H$(p, p')pn$, which is considered to be a continuation of the elastic scattering.
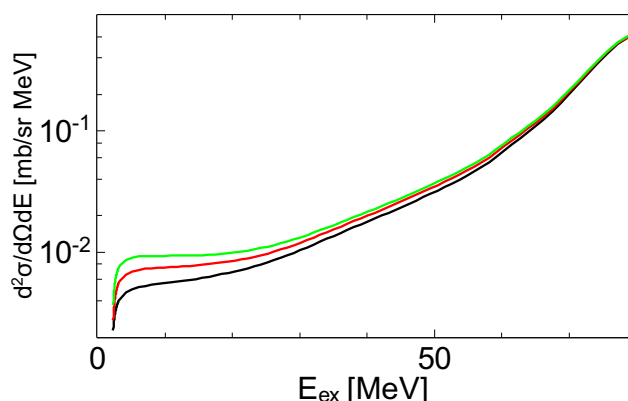
Figure 3: Cross section for inclusive breakup reaction, ^{2}H$(p, p')pn$, for proton scattering angle 110° at $E_p = 170$ MeV as a function of excitation energy of the residual pn system. Black, red, and green curves denote AV18, AV18+BR$_{660}$, and AV18+BR(C)$_{1000}$ calculations, respectively.

In Fig. 3, cross sections of the ^{2}H$(p, p')pn$ reaction for proton scattering angle in laboratory system to be 110° at $E_p = 170$ MeV. This angle corresponds to 140° at c.m. system in the p-d elastic scattering, where the effect the BR(C)$_{1000}$-3NP is remarkable as shown in Fig. 2 (b). The cross sections for AV18, AV18+BR$_{660}$, and AV18+BR(C)$_{1000}$ are plotted as functions of the excitation energy of the residual p-n system E_{ex}, which is 0 for the elastic scattering. Effects of the large cutoff parameter in the 2πE-3NP, which are shown by the difference between the red curve and the green curve are well visible.

3.3 Cutoff in coordinate space

Since the use of the dipole form factor is not unique way to suppress a short-range part of interactions, I will examine other method: one used in recent the chiral effective field theory (χEFT). In recent calculations of few- and many-nuclear systems [10–12], 2NPs based on χEFT are provided in the coordinate space representation with multiplying a damping function (called as regulator) $f_R(r)$, where R is a parameter representing the range of cutoff. The cutoff procedure used in constructing the 2NP is also applied to 3NP as follows:

$$V_R^{(3:1,2)}(\vec{r}_{13}, \vec{r}_{23}) = f_R(r_{13})f_R(r_{23}) \times \int d\vec{q}_1 d\vec{q}_2 e^{-i\vec{q}_1 \cdot \vec{r}_{13} - i\vec{q}_2 \cdot \vec{r}_{23}} \hat{V}^{(3:1,2)}(\vec{q}_1, \vec{q}_2). \tag{5}$$

In the present work, two different functional forms of the regulator will be used. One, which will be designated as [I], is from Refs. [10, 11]:

$$f_R^{[I]}(r) = \left[1 - \exp\left(-\frac{r^2}{R^2}\right)\right]^6, \tag{6}$$

and the other, which will be designated as [II], is from Ref. [12]:

$$f_R^{[II]}(r) = 1 - \frac{1}{(r/R)^6 e^{(r-R)/(R/2)} + 1}. \tag{7}$$

First, the range parameters are decided to reproduce the ^{3}He binding energy, and the results with the BR07-3NP are $R = 0.87$ fm for [I] and $R = 1.29$ fm for [II]. The regulators with these parameters as functions of r are plotted by black solid curve for $f_R^{[I]}(r)$, and black
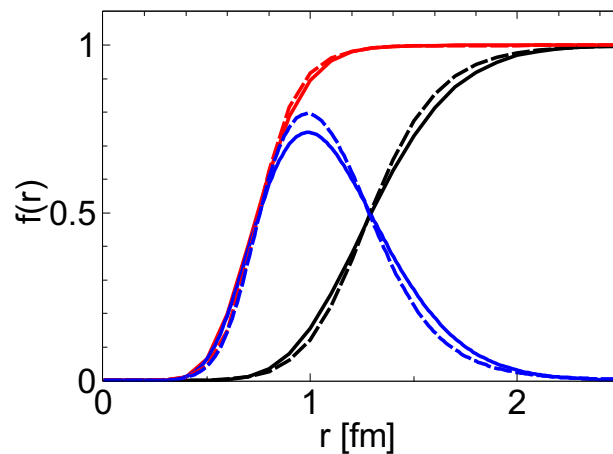
Figure 4: The regulator functions, Eq. (6) and Eq. (7). The meaning of the curves are described in the text.

dashed curve for $f_R^{[I]}(r)$ in Fig. 4. Range of the regulator may be characterized by a value of $r_{0.5}$ that satisfies $f_R(r_{0.5}) = 0.5$. For both of $f_{R=0.87}^{[I]}(r)$ and $f_{R=1.29}^{[II]}(r)$, $r_{0.5}$ becomes about 1.3 fm, which indicates a long-range character of the regulators.

Next, in order to make the BR07-3NP more attractive, the range parameter R for each of the regulator is changed to be smaller value so that $r_{0.5} \approx 0.75$ fm, which gives $R = 0.5$ fm for [I] and $R = 0.75$ fm for [II]. As in the case of the dipole form factor, I will introduce the repulsive C-3NP to reproduce the ^{3}He binding energy. The strength parameters of the C-3NP are shown as $BR(C)_{[I]0.5}$ and $BR(C)_{[II]0.75}$ in Table 1.

In Fig. 5, calculations of p-d scattering at $E_p = 170$ MeV for AV18+BR(C)$_{[I]0.5}$, AV18+BR(C)$_{[II]0.75}$ as well as AV18+BR(C)$_{1000}$ are plotted. This figure shows a similarity among AV18+BR(C)$_{[I]0.5}$, AV18+BR(C)$_{[II]0.75}$, and AV18+BR(C)$_{1000}$ calculations, and these calculations almost equally resolve the difference between the data and calculations. This indicates that the regulator functions $F_{R=0.5}^{[I]}(r)$ and $F_{R=75}^{[II]}(r)$ play a similar role as the form factor with $\Lambda = 1000$ MeV in the 2πE-3NP.

In Fig. 4, the functions $F_{R=0.5}^{[I]}(r)$ and $F_{R=0.75}^{[II]}(r)$ are plotted as red solid curve and red dashed curve, respectively. In the figure, the differences between $F_{R=0.5}^{[I]}(r)$ and $F_{R=0.87}^{[I]}(r)$, and $F_{R=0.75}^{[II]}(r)$ and $F_{R=1.29}^{[II]}(r)$ are plotted as blue solid curve and blue dashed curve, respectively, which demonstrates that the increase of the p-d cross sections at minimum and backward angle regions is caused by effects of the pion-exchange around $r = 1$ fm.

4 Conclusion

The use of a larger value of cutoff parameter in the form factor, or a short range cutoff of the regulator in the 2πE-3NP enhances p-d elastic cross sections at backward angles for intermediate energies, which tends to reduce the discrepancies between data and calculations. Similar effects are observed in inclusive breakup reactions. This demonstrates the importance of pion exchange in the 2πE-3NP around $r = 1$ fm.

In this work, the repulsive 3NP to compensate the large attractive effect of the 2πE-3NP is introduced phenomenologically. Physical origin of it as well as spin-dependence of 3NPs to reproduce polarization observables in p-d scattering are left as future problems.

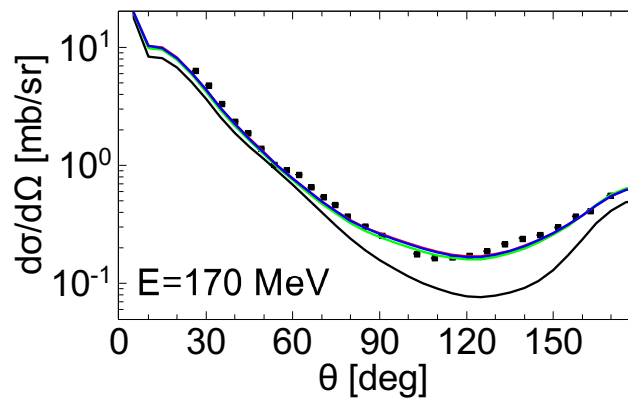Figure 5: Cross sections for *p-d* elastic scattering at $E_p = 170$ MeV. Black, green, blue, and cyan curves denote AV18, AV18+BR(C)$_{1000}$, AV18+ AV18+BR(C)$_{[I]0.5}$, and AV18+BR(C)$_{[II]0.75}$ calculations, respectively. The latter three curves are almost overlapped mutually. Experimental data are taken from Ref. [8].

References

[1] S. Ishikawa, *Two-pion exchange three-nucleon force effects in elastic nucleon–deuteron scattering cross sections*, Few-Body Syst. **60**, 39 (2019), doi:10.1007/s00601-019-1506-z.

[2] L. D. Faddeev, *Scattering theory for a three-particle system*, Zh. Eksp. Teor. Fiz. **39**, 1459 (1961) http://www.jetp.ac.ru/cgi-bin/e/index/e/12/5/p1014?a=list.

[3] S. Ishikawa, *Coordinate space proton-deuteron scattering calculations including Coulomb force effects*, Phys. Rev. C **80**, 054002 (2009), doi:10.1103/PhysRevC.80.054002.

[4] S. Ishikawa and M. R. Robilotta, *Two-pion exchange three-nucleon potential: $O(q^4)$ chiral expansion*, Phys. Rev. C **76**, 014006 (2007), doi:10.1103/PhysRevC.76.014006.

[5] R. B. Wiringa, V. G. J. Stoks and R. Schiavilla, *Accurate nucleon-nucleon potential with charge-independence breaking*, Phys. Rev. C **51**, 38 (1995), doi:10.1103/PhysRevC.51.38.

[6] R. Machleidt, *High-precision, charge-dependent Bonn nucleon-nucleon potential*, Phys. Rev. C **63**, 024001 (2001), doi:10.1103/PhysRevC.63.024001.

[7] H. Shimizu, K. Imai, N. Tamura, K. Nisimura, K. Hatanaka, T. Saito, Y. Koike and Y. Taniguchi, *Analyzing powers and cross sections in elastic p-d scattering at 65 MeV*, Nucl. Phys. A **382**, 242 (1982), doi:10.1016/0375-9474(82)90134-8.

[8] K. Ermisch et al., *Systematic investigation of the elastic proton-deuteron differential cross section at intermediate energies*, Phys. Rev. C **68**, 051001 (2003), doi:10.1103/PhysRevC.68.051001.

[9] S. Ishikawa, M. Tanifuji and Y. Iseri, *Central and tensor components of three-nucleon forces in low-energy proton-deuteron scattering*, Phys. Rev. C **67**, 061001 (2003), doi:10.1103/PhysRevC.67.061001.

[10] S. Binder et al., *Few-nucleon and many-nucleon systems with semilocal coordinate-space regularized chiral nucleon-nucleon forces*, Phys. Rev. C **98**, 014002 (2018), doi:10.1103/PhysRevC.98.014002.

[11] E. Epelbaum et al., *Few- and many-nucleon systems with semilocal coordinate-space regularized chiral two- and three-body forces*, Phys. Rev. C **99**, 024313 (2019), doi:10.1103/PhysRevC.99.024313.

[12] M. Piarulli et al., *Light-nuclei spectra from chiral dynamics*, Phys. Rev. Lett. **120**, 052503 (2018), doi:10.1103/PhysRevLett.120.052503.